Composites Part B 93 (2016) 352–359

Contents lists available at ScienceDirect

Composites Part B

journal homepage: www.elsevier.com/locate/compositesb

Laser sintered single layer graphene oxide reinforced titanium matrix nanocomposites

Zengrong Hu [a, b, c, *], Guoquan Tong [a, **], Qiong Nian [e], Rong Xu [d], Mojib Saei [e], Feng Chen [a], Changjun Chen [b], Min Zhang [b], Huafeng Guo [a, f], Jiale Xu [c]

[a] College of Mechanical and Electrical Engineering, Nanjing University of Aeronautics and Astronautics, Nanjing, Jiangsu 210016, China
[b] School of Urban Rail Transportation, Soochow University, Suzhou, Jiangsu 215131, China
[c] Jiangsu Provincial Key Laboratory for Science and Technology of Photon Manufacturing (Jiangsu University), Jiangsu 212013, China
[d] School of Mechanical Engineering, Purdue University, West Lafayette, IN 47906, USA
[e] School of Industrial Engineering, Purdue University, West Lafayette, IN 47906, USA
[f] Xuzhou Institute of Technology, Xuzhou, Jiangsu 221111, China

ARTICLE INFO

Article history:
Received 1 September 2015
Received in revised form
1 February 2016
Accepted 13 March 2016
Available online 19 March 2016

Keywords:
A. Metal-matrix composites (MMCs)
A. Particle-reinforcement
B. Hardness
E. Sintering

ABSTRACT

Single layer graphene oxide (SLGO) reinforced titanium (SLGO-Ti) nanocomposites have been achieved by laser sintering. This study focuses on the graphene oxide dispersion and survival in titanium matrix during laser sintering process. Through laser sintering, graphene oxides were dispersed uniformly into titanium matrix to fabricate SLGO-Ti nanocomposites. Microstructures and components of the nanocomposites were studied using scanning electron microscopy (SEM), X-ray diffraction (XRD), Energy-dispersive X-Ray spectroscopy (EDS) and Raman spectroscopy. It was confirmed by XRD patterns, EDS maps and Raman spectrum that graphene oxide survived in SLGO-Ti nanocomposites after laser sintering. Nanoindentation measurements showed the laser sintered SLGO-Ti nanocomposites hardness was improved by more than 3-folds than that of pure titanium counterpart.

1. Introduction

Titanium (Ti) and titanium alloy are widely used in various fields like biomedical, aerospace and automobile industries, due to their outstanding specific strength, toughness and the ability to withstand higher temperature than steel and aluminum alloy. However, utilization of titanium and titanium alloy in many fields requires even higher strength and thermal conductivity, especially in aerospace field. In fact, some applications are also limited for their poor thermal conductivity [1]. It is well known that composites which are made from two or more constituent materials have many attractive properties, and can be much stronger, lighter and with improved thermal and electrical properties when compared with traditional intrinsic materials. Nanocomposites become more and more attracting, especially metal matrix nanocomposites which are considered as infrastructure materials for its outstanding properties, such as high hardness, high specific stiffness, low coefficient of thermal expansion, high yield strength, anti-corrosion property, and creep resistance in high temperature environment etc. [2]. Therefore, plenty of research works have been carried out to study different sorts of metal matrix composites (MMCs) and nanocomposites. Various nanoparticles have been considered as composite filler materials, especially carbon nanotubes (CNTs) and graphene [3–8].

Graphene, with demonstrated high strength and thermal conductivity [9], has the potential to serve as a reinforcement for improving not only mechanical but also thermal properties of titanium and titanium alloy. Graphene is just one layer carbon atom thick sheet, in which carbon atoms form flat honeycomb lattice. The special structure brings exceptional properties, such as high electric property [10], high Young's modulus [11], outstanding tribological property [12,13], and high tensile stress [14], besides the superior thermal conductivity. Thereby, it is expected that graphene-titanium composites would have superior thermomechanical properties. Recently, a few graphene reinforced metal matrix nanocomposites have been studied [15–20]. These research works showed great promise to enhance the properties of metal matrices. However, it is extremely difficult to disperse graphene homogeneously in metal

* Corresponding author. School of Urban Rail Transportation, Soochow University, Suzhou, Jiangsu 215131, China.
** Corresponding author.
E-mail address: zengronghu@126.com (Z. Hu).

http://dx.doi.org/10.1016/j.compositesb.2016.03.043
1359-8368/

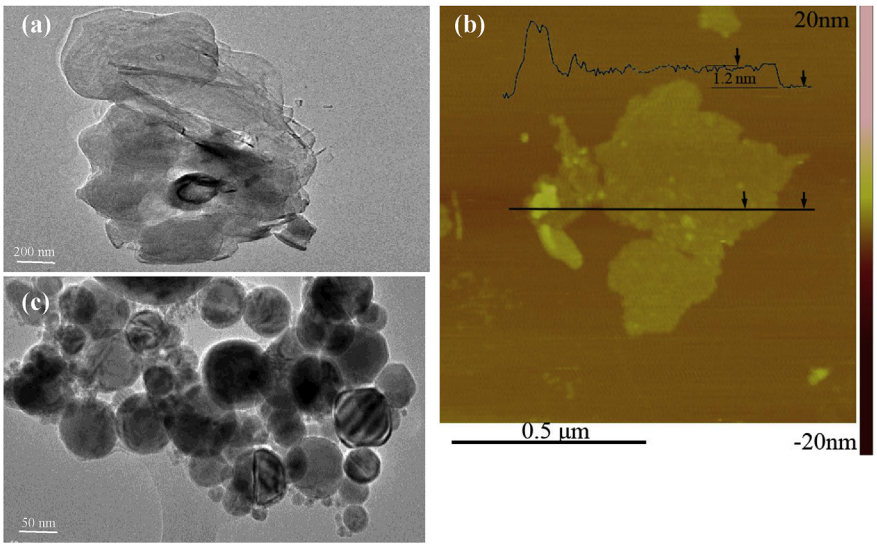

Fig. 1. (a) TEM image of SLGO, (b) AFM image of SLGO, (c) TEM image of Ti-SLGO before laser sintering.

matrix [4]. It is even more difficult to make graphene reinforced titanium nanocomposites, since titanium is an active metal can react with carbon easily.

Graphene oxide (GO), a graphene derivative, is mono-layer of sp^2-hybridized carbon atoms derivatized by a mixture of carboxyl, hydroxyl and epoxy functionalities [21]. It is well known that GO can be easily dispersed in water, because of the oxygen functional groups, attached on the basal planes and edges of GO sheets, which significantly alter the van der Waals interaction between the GO sheets. GO has similar mechanical properties with graphene, which exhibits high tensile strength [22] and less possibility to react with titanium matrix due to the passivation of functional groups. In addition, GO can be mass-produced from graphite oxide with low costs. These virtues make it an ideal reinforcement for nanocomposites. It was reported that addition of 1wt.% GO could simultaneously improve the strength and toughness of GO-chitosan composites [23]. And for GO-cement composites, 0.05% GO sheets improve the compressive strength and flexural strength by 15–33% and 41–58%, respectively [24]. For metal matrix composites, GO-iron composites were reported in 2014, the surface microhardness of laser sintered 2 wt. % GO-iron composite was 600 HV, which has increased 93.5% compared with the base material [7]. To date, to the best of our knowledge, there is still no report of GO reinforced titanium matrix composites.

Herein, a laser sintering technique was used to fabricate graphene oxide reinforced titanium nanocomposites. Laser sintering is a rapid heating and rapid cooling process, which helps to keep graphene oxide in the titanium matrix from reacting with the matrix. At the same time, graphene oxide melting point is over 3000 °C [25], and titanium nanopowders melting point is 1660 °C (even lower melting point of Nano size Ti powder) [26], which also helps graphene oxide survive in the laser sintering process.

Single layer graphene oxide nanoplatelets were mixed with titanium nanopowders in deionized water, ultrasonic dispersing for 1 h. Then the mixed solution was dipped on mechanically polished AISI 4140 substrate surface [27–29], after natural air drying, a thin layer of graphene oxide and titanium mixture was coated. The layer thickness can be controlled by coating times, and the volume ratio of graphene oxide and titanium also can be controlled easily. Finally, laser was used to sinter the coatings, which were put into a transparent chamber filled with argon gas to protect titanium from oxidation or nitridation. Afterwards, SLGO-Ti nanocomposites were successfully deposited. It was expected that the nanocomposites would have excellent mechanical properties.

2. Experiments

Materials: The substrates AISI 4140 plate was cut into small pieces of 10 mm × 8 mm × 2.35 mm. The titanium powders (average diameter 30–50 nm) and single layer graphene oxide (thickness 0.7–1.2 nm, average X&Y dimension 300–800 nm, Cheap Tubes, Inc.) were used for the experiment. Fig. 1a is the TEM image of SLGO, and Fig. 1b is the AFM image of SLGO. It can be seen from Fig. 1b that the thickness of SLGO is 1.2 nm, and its size is about 600 nm.

Laser sintering experiments: Ti nanopowders and SLGO nanoplatelets were used to make two kinds of solution by ultrasonic dispersion. Firstly, mix 1.9 g Ti nanopowders, 0.1 g SLGO nanoplatelets and 23 g deionized water; secondly, 2.0 g Ti nanopowders and 23 g deionized water, respectively, ultrasonic dispersed it for 1 h. Fig. 1c is the TEM image of Ti-SLGO before laser sintering. The AISI 4140 samples were first ultrasonically cleaned and mechanical polished to a surface roughness about 0.05 μm [5–8,30]. Then the samples were coated several times with the previous prepared suspension by using a dropper, until the dried coating layer thickness reached 0.2 mm. Fig. 2a shows the schematic cross-section after coating. An IPG fiber pulse laser (wave length: 1064 nm, pulse duration: 400 ns) system was used to perform the laser sintering process at the frequency of 50 kHz. The selected laser parameters were: laser intensity (80 W), beam size (0.8 mm), scanning speed (2 mm/s) and step size (0.25 mm). The coverage area was the whole sample surface, as shown in Fig. 3. The samples were sintered in a transparent chamber filled with Argon (Ar) gas which protected the samples from oxidation and nitridation during laser sintering process. The chamber was fixed on a numerical controlled (NC) x-y stage. Fig. 2b represents the schematic cross-section after laser sintering. With proper technical parameters, the graphene oxide nanoplatelets survived and were distributed uniformly in the titanium matrix after laser sintering process. The coated layer was melted together with substrate by laser sintering.

Microstructure characterization: A Bruker D8 Focus X-Ray diffractometer was used to characterize the material composite with Cu-Kα source. Laser sintered samples were prepared for XRD

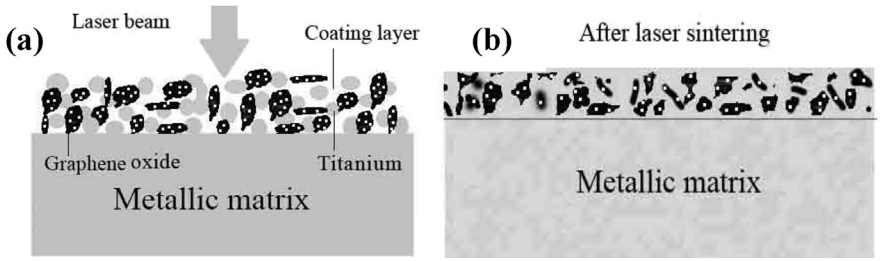

Fig. 2. Schematics of laser sintering of SLGO-Ti pre-coated on substrate. Schematic cross-section of the sample (a) after surface coating and (b) after laser sintering.

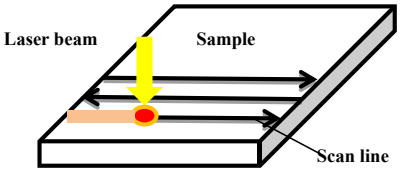

Fig. 3. Schematics of laser sintering process.

measurement. A Hitachi S-4800 Field emission SEM was used to study the surface morphology and cross-sectional microstructures. The Raman spectra were obtained by a HORIBA LabRAM HR800 Raman spectrometer (HORIBA Jobin Yvon, NJ, USA). A 632.8 nm He-Ne laser was focused by an Olympus 50 × objective (MPLN50x, Olympus America) as an excitation source, at the center of the sample placed in an open air environment at room temperature.

Mechanical property testing: The laser sintered SLGO-Ti samples were measured by Agilent Nano indenter G200. The micro-hardness of laser sintered Ti and SLGO-Ti nanocomposites, were measured by Leco M-400-H micro-hardness instrument with 200 g load and 10s holding time. The metallographic polishing machine was used to polish the samples surfaces by removing a very thin layer in order to measure the micro-hardness. All the tests were carried out at room temperature and in a laboratory environment.

3. Results and discussion

3.1. Microstructure of laser sintered SLGO-Ti nanocomposites and Ti

Fig. 4a and b show the SEM images of surface morphology of laser sintered SLGO-Ti nanocomposites and Ti. It can be observed from the SEM images that both Fig. 4a and b have a rough surface morphology. The particles on Fig. 4a are bigger than those on Fig. 4b, and the number of particles is less. This means during laser sintering process, when Ti nanopowders melted and re-solidified with SLGO, and SLGO did not melt in the laser sintering process. The solid state SLGO nanoplatelets would draw liquid Ti, to makes the surface flat and make some particles size become bigger. That is partly the reason for the laser sintered SLGO-Ti generally has a flatter surface morphology than laser sintered Ti which has gaps and small high regions. This also may be because small SLGO platelets were connected with each other to form a whole frame, and it helped to joint the melt Ti during the laser sintering process. This made the whole surface flat when the liquid titanium solidified with SLGO. From the cross section SEM images of Fig. 4c and d, it can be observed that laser sintered SLGO-Ti nanocomposite seems to have finer grains than that of laser sintered Ti. It may be because graphene oxide nanoplatelets can inhibit grain growth through grain boundary pinning and a diffusion barrier of other elements [31]. It was also consistent with XRD results. From Fig. 5, it can be seen that the width of Ti peaks are different in the two XRD patterns. The widths of Ti peaks in SLGO-Ti XRD pattern are bigger than those of corresponding peaks in Ti XRD pattern. This means SLGO-Ti nanocomposites had finer grain than that of laser sintered Ti.

3.2. XRD analysis

XRD was used to characterize the phase and structure of the laser sintered SLGO-Ti nanocomposites and Ti. Fig. 5 shows the XRD patterns of SLGO-Ti nanocomposites and Ti. SLGO-Ti XRD pattern has a peak at 2θ degree of 26.5°, which can be indexed into the carbon element of graphene oxide sheets. After laser sintering, Ti XRD pattern also shows a very small peak at 26.5°, which might be attributed to the carbon come from AISI 4140 substrate.

The other diffraction peaks can be indexed as titanium and iron. The iron exists in laser sintered Ti and SLGO-Ti nanocomposites, because the substrate plate is AISI 4140, which has a high ratio component of iron. From Fig. 5, it can be found that there are no oxidations and carbides diffraction peaks which mean the Ar gas effectively protected the laser sintering process and graphene oxide survived during laser sintering.

3.3. EDS analysis

Fig. 6a is the cross section SEM image of SLGO-Ti nanocomposites. It can be found graphene oxide exists in the composite which are marked on the image. Fig. 6b–d is EDS maps of titanium, oxygen and carbon in the cross section. In fact, it can be seen that the distribution of oxygen, which mainly came from the functional groups of GO, was not uniform. It was also not consistent with carbon maps. The explanations are: as it was well known that GO may be reduced to graphene due to the pyrolysis of oxygen-containing functional groups such as hydroxyl, carbonyl, and carboxylic acid to yield CO, CO_2, and H_2O, when it was heated to a certain temperature [32,33]. Although, fast heating and cooling laser sintering process made GO survive, at the same time it was inevitably made them partly lose functional groups or made a small part of GO converted to reduce GO. That means for this part of SLGO, which lost or partly lost oxygen-containing functional groups, the carbon was still there but the oxygen was lost. This is the reason for the inconsistency of carbon and oxygen maps. There were no GO clear-cut shapes on the titanium, carbon and oxygen EDS maps. But on the carbon map, it can be found, the yellow ellipses marked areas, corresponding to the marked GO areas on Fig. 5a, the carbon intensity was a little higher than that of other area. Remember, the GO used in this project was SLGO, and they were dispersed very uniformly, meanwhile the volume content of GO in the composites was high. This can partly explain the almost uniform distribution of those elements in EDS maps. And it is well known that EDS detecting depth affected by various factors, such as accelerating voltage, element type etc. The EDS equipment will detect deeper when the atomic number of detected element is small. Relatively, the atomic number of Ti is small, so the detected

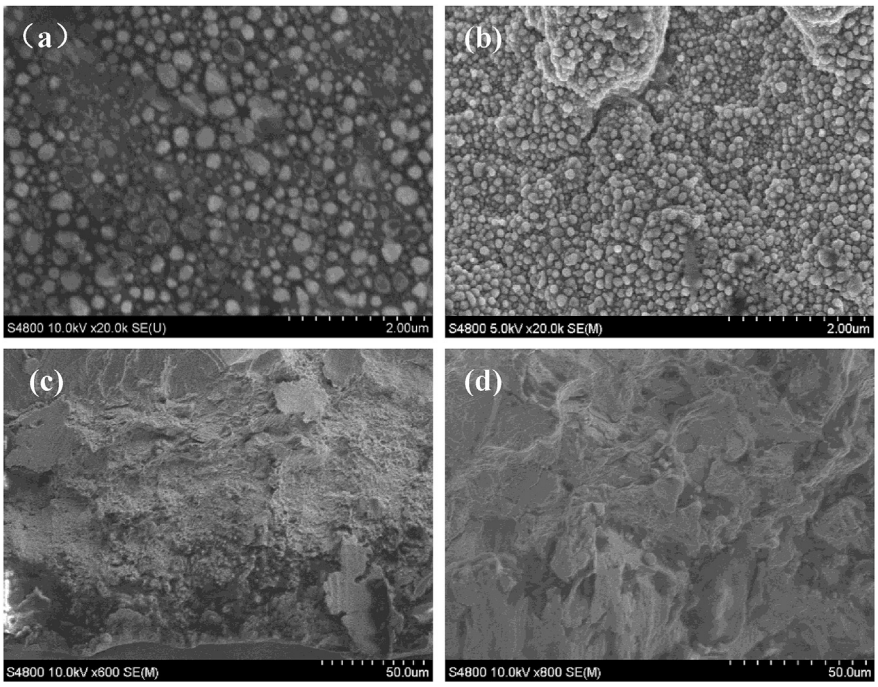

Fig. 4. SEM images of surface morphology of (a) laser sintered 5wt. % SLGO-Ti nanocomposites and (b) laser sintered Ti, (c) cross section of laser sintered 5wt. % SLGO-Ti nanocomposites and (d) cross section of laser sintered Ti.

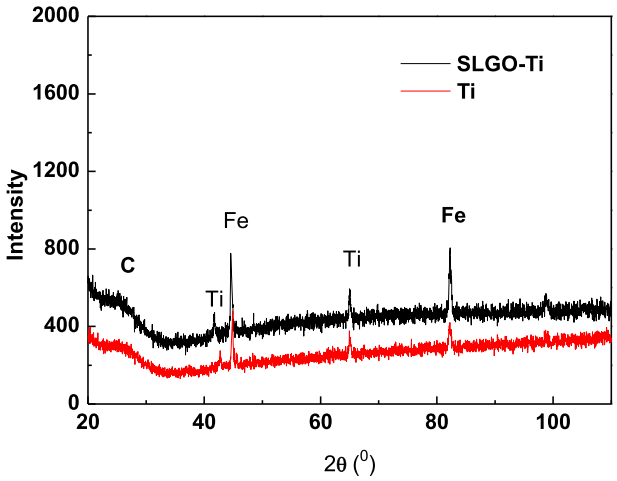

Fig. 5. The XRD patterns of laser sintered 5wt. % SLGO-Ti nanocomposites and Ti.

depth may be more than 3 μm in this measurement. That means the EDS maps reveal the elements distribution of at least this whole 3 μm thick layer. This may explain why there is no SLGO clear-cut shape on the titanium, carbon and oxygen EDS maps. Because one layer or several layers of SLGO on the cross section had no significant effect on the elements EDS maps, it would only make a very slight difference.

3.4. Raman spectrum analysis

Raman spectroscopy was used to characterize laser sintered SLGO-Ti nanocomposites. Fig. 7 shows the Raman spectra of laser sintered SLGO-Ti nanocomposites and SLGO-Ti coating before laser sintering process. It can be clearly seen from Fig. 7a, Raman spectrum of laser sintered SLGO-Ti nanocomposite shows the peaks at ~1341, ~1586 cm^{-1}, corresponding to the D peak and G peak of graphene oxide, respectively, while Raman spectrum of SLGO-Ti coating show the peaks at ~1332, ~1594 cm^{-1} [34], corresponding to the D peak and G peak of SLGO. Comparing the two Raman spectra, it can be found that the positions of D and G peaks were slightly changed after laser sintering process. This phenomenon can be found in graphene reinforced metal matrix composites [35]. But the shape of D and G peaks were similar, and the I_D/I_G value almost had no change.

From Fig. 7, it can be found that, after laser sintering, the intensity of Raman spectrum was decreased significantly, it might be because after solidified with melt titanium, graphene oxide becomes difficult to detect and/or during the laser sintering process, some of graphene oxide were damaged or lost, but it does exist in the nanocomposites.

3.5. Mechanical properties of laser sintered SLGO-Ti nanocomposites and Ti

Hardness and modulus are commonly used to assess the composites strengthened results. Nano-indentation was a well-developed method for composites nanomechanical properties test. Fig. 8a is the nanoindentation load – penetration depth curves randomly measured on the polished surface of laser sintered Ti and SLGO-Ti nanocomposites samples. Three different points were measured on each sample, loading and unloading 5 times at each point. The loading force increased every time, with 90% unloading of previous loading force. Comparing laser sintered Ti load – penetration depth curves with that of SLGO-Ti nanocomposites, it can be found that under the same load, Ti samples had much deep penetration depth into the surface. This means the strength and hardness of laser sintered Ti is lower than that of laser sintered SLGO-Ti nanocomposites. The fabricating parameters for both kinds of materials were the same; it indicated that the improvements were due to graphene oxide reinforcement.

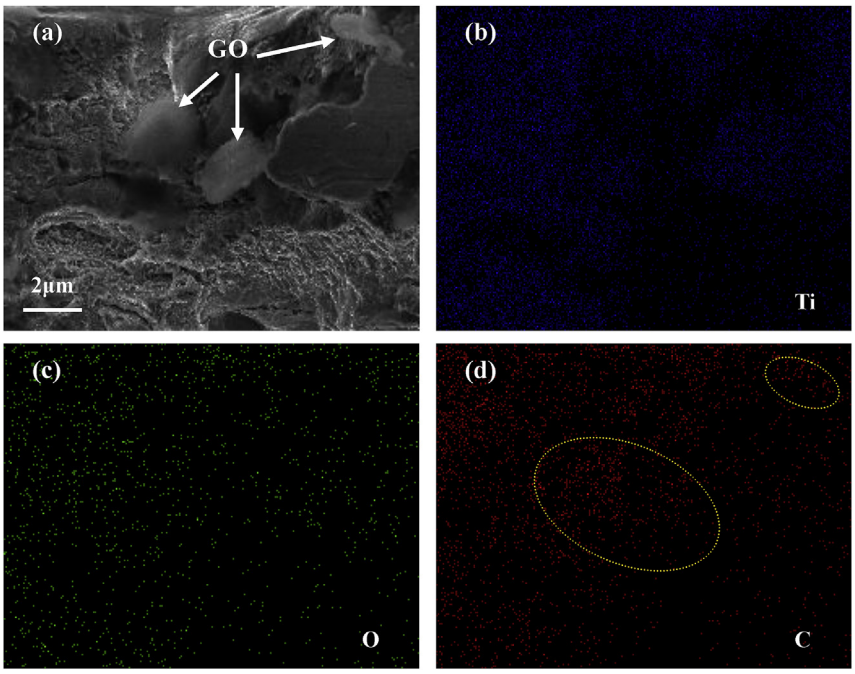

Fig. 6. (a) SEM image of the cross section of 5wt. % SLGO-Ti nanocomposites, (b), (c) and (d) are Ti, O, C EDS maps of (a).

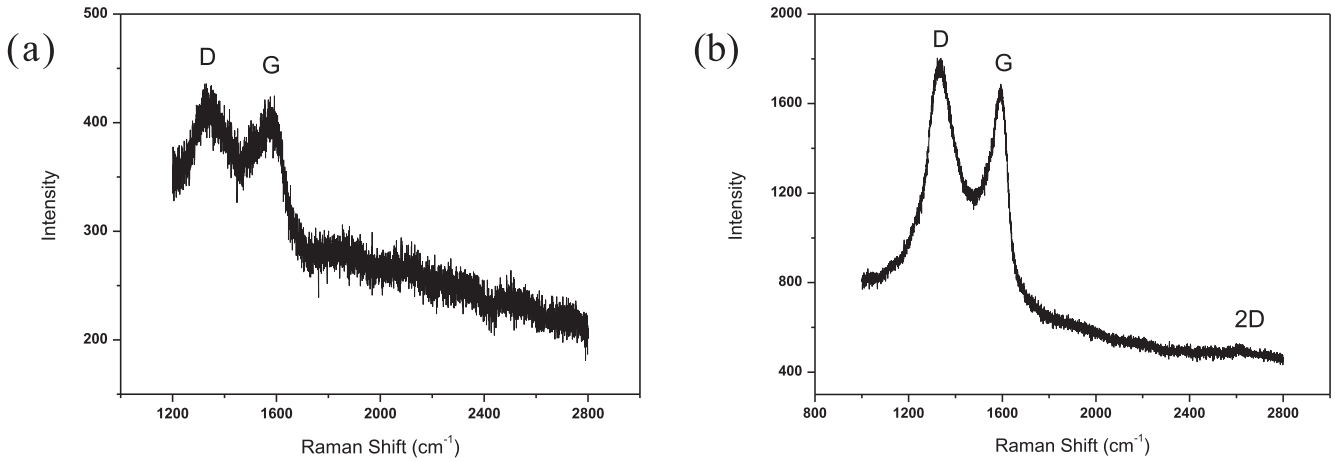

Fig. 7. Raman spectra of (a) laser sintered 5wt. % SLGO-Ti nanocomposites, and (b) 5wt. % SLGO-Ti coating before laser sintering.

Fig. 8b is the hardness – penetration depth curves of laser sintered Ti and SLGO-Ti nanocomposites samples measured by nanoindenter. It can be seen that the hardness of laser sintered Ti is uniform and the average value is about 3.5 GPa, which is consistent with other report [36]. At the same time laser sintered SLGO-Ti nanocomposites have an average hardness value of about 11 GPa, the improvement is significant, but the hardness values are not as uniform as that of Ti's. It may be because the indenter tip is tiny and if the measuring position was located on, or near the SLGO sheets, the high hardness value will be got, and otherwise low hardness value will be got. As well know, hardness is a comprehensive performance of strength and resistance to deformation, friction and abrasion. The improvement on hardness means it was well strengthened.

Fig. 8c is the modulus – penetration depth curves. They almost have the same tendency with the hardness – penetration depth curves. In fact, normally, materials which have high hardness should also have high modulus [37]. It can be found from Fig. 8c that the average modulus value of laser sintered Ti is about 125 GPa, and the average modulus value of laser sintered SLGO-Ti nanocomposites is about 200 GPa. Modulus increase was mainly attributed to the high modulus of single layer graphene oxide.

The 1wt. %, 2.5wt. % and 5wt. % SLGO-Ti nanocomposite samples were made under the same condition. Fig. 8d shows the Vickers hardness values of laser sintered SLGO-Ti nanocomposites as a function of SLGO weight percentage. The hardness values were averaged on 5 point measurements on each sample. Fig. 8d clearly shows the hardness values of laser sintered 1wt.% SLGO-Ti(630VH), 2.5wt.% SLGO-Ti (742VH) and 5wt.% SLGO-Ti (509VH), the highest value is 4-fold more than that of the laser sintered Ti (180VH). It should be noticed that with the addition of SLGO, the hardness of laser sintered SLGO-Ti improved significantly. As the SLGO content increasing, the hardness improvement also increased, after certain SLGO content value, further increasing SLGO content would reduce

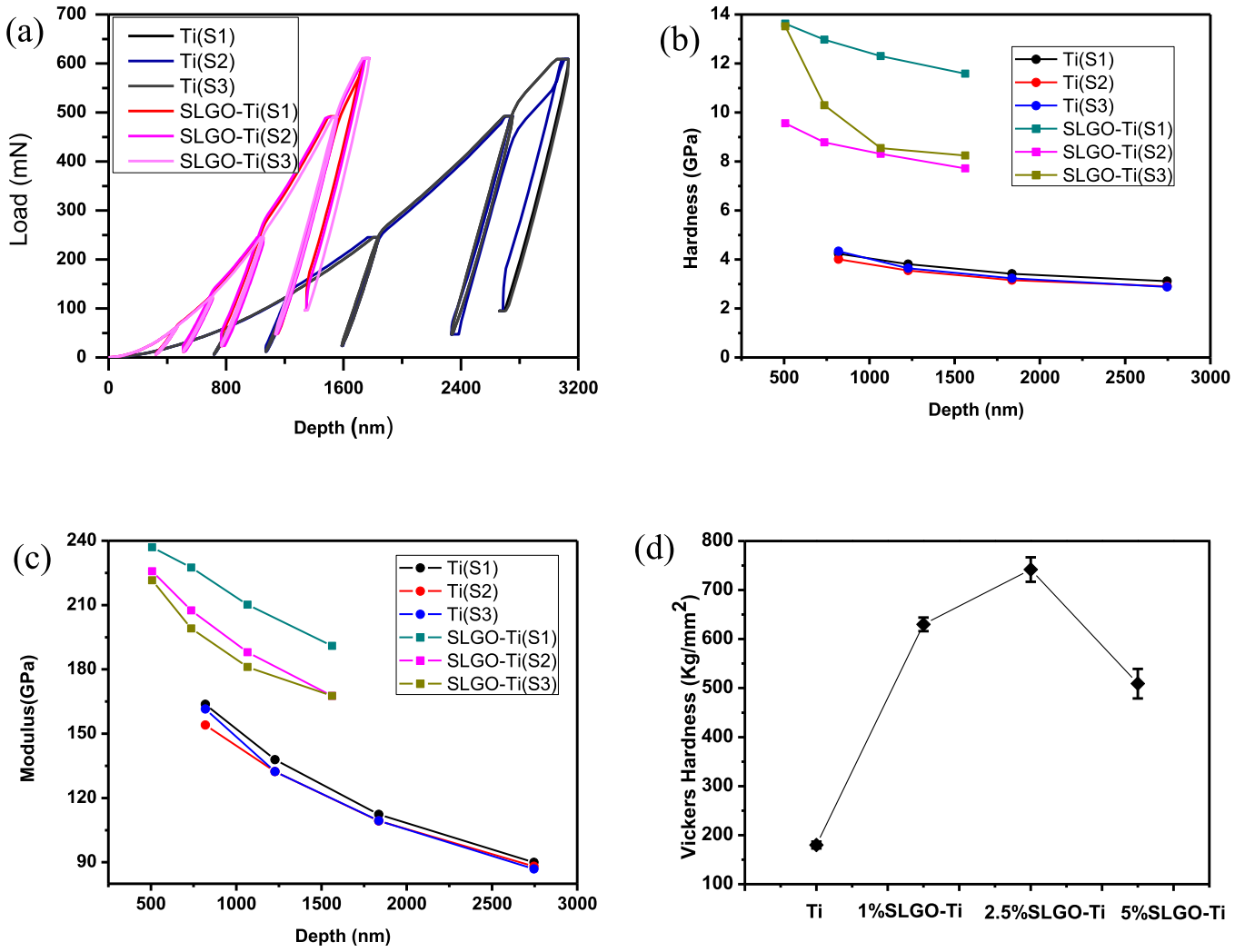

Fig. 8. Laser sintered 5wt. % SLGO-Ti nanocomposites and Ti (a) Load– penetration depth curves, (b) hardness – penetration depth curves, (c) modulus – penetration depth, and (d) Vickers hardness.

hardness improvement. It may be because of the aggregation of SLGO. Although, compared with graphene, GO is easier to disperse into metal powder, it will still aggregate. It was said that the hardness improvement mainly attribute to the excellent mechanical properties of SLGO [38]. During the material deformation, SLGO fillers will carry the load and pinning dislocation movement. It was well known that SLGO was 2D material, similar with graphene whose out-of-plane properties is significantly lower than that of in-plane properties [39], so the bonding force between SLGO layers was weak. When the content increases, SLGO is easy to pile up, and also easy to form pore in the composites [15], these could be employed to explain the hardness improvement changes with the content increasing. In fact similar phenomenon can be found in the graphene-copper research work reported by Chu and Jia [38].

3.6. Strengthening mechanisms of SLGO-Ti nanocomposites

Generally, the metal material which has higher hardness also has higher strength [37]. The hardness measurement results of different SLGO-Ti nanocomposites and nanoindentation measurement results showed great improvement had been achieved. The mainly strengthening mechanisms are: reinforcement filler strengthening, dislocation strengthening, and fine grain strengthening.

Reinforcement filler strengthening is the main strength mechanism, because the filler material SLGO has excellent mechanical properties. According to the mixing law which can be expressed by the following equation:

$$\sigma_c = \sigma_m V_m + \sigma_g V_g \quad (1)$$

Where σ_c, σ_m, σ_g is SLGO-Ti nanocomposites strength, Ti matrix strength and SLGO strength, respectively. V_m and V_g are the volume ratios of Ti matrix and SLGO. Although, this equation is simple and not precise, it still can be used to estimate the composites properties. Generally, it is right that the stronger filler have better strength effect.

Dislocation strengthening, as we know, dislocation can strengthen nanocomposites. The dislocation density will increase when the nano-filler size decreases and the volume fraction increases [40]. In this study the nano size SLGO platelets would cause the dislocation density increased in the SLGO-Ti nanocomposites. And after laser sintering, the relaxation of thermal residual could also increase the dislocation density [41], which can be calculated by Ref. [42].

$$\Delta\rho = \frac{\Delta\alpha\Delta T N A}{b} \quad (2)$$

Where ΔαΔT is thermal misfit strain, N is the nanoparticles number, b is the Burger's vector and A is the total surface of each nanoparticle.

In SLGO-Ti nanocomposites, SLGO could pin the dislocation, through hinder dislocation movement to strengthen the composites, it was known as Orowan strengthening [43]. The dislocation density also influences the micro hardness of composites, the relationship can be described by

$$H = H^* + \alpha G b\sqrt{\rho} \quad (3)$$

Where H^*, α, G are material's constants, b is Burger's vector and ρ is the dislocation density [44].

Fine grain strengthening mechanism is often called Hall-Petch strengthening. The enhancement is achieved by refining the composites grain size and hindering dislocation movement by grain boundaries. The Hall-Petch strengthening can be described by Ref. [45].

$$\Delta\sigma_{H-P} = \frac{k_y}{\sqrt{d}} \quad (4)$$

Where k_y is the strengthening coefficient (characteristic constant of each material) and d is the average diameter of grain size. As mentioned above, SLGO nanoplatelets can refine the composites grain size; therefore it strengthens the nanocomposites.

4. Conclusions

The 1wt. %, 2.5wt. %, 5wt. % SLGO reinforces titanium nanocomposites were first prepared by laser sintering in this work. Compared with other graphene or graphene oxide reinforced metal matrix nanocomposites fabrication technologies, laser sintering is fast, flexible and economical.

It was proved by XRD test and Raman spectra that SLGO survived in the laser sintered composites. After laser sintering process, SLGO was mixed into the titanium matrix to form SLGO-Ti nanocomposites. The SEM images give the surface and cross section morphology of the two kinds of samples. Cross section SEM image showed graphene oxide was dispersed in the composite. The SLGO-Ti nanocomposites showed a very high hardness value and modulus value than that of laser sintered Ti. The average nano-indentation hardness value of the nanocomposites (11GPA) is more than 3-fold higher than that of laser sintered titanium (3.5 GPa). Meanwhile the average modulus value of the nanocomposites also has a notable increase. The Vickers hardness values of laser sintered 1wt. % SLGO-Ti (630VH), 2.5wt. % SLGO-Ti (742VH) and 5wt. % SLGO-Ti (509VH) indicated that SLGO is a promising reinforcement material for titanium and, there is an optimal SLGO content for laser sintered SLGO-Ti nanocomposites.

Acknowledgments

This work was supported by the Open Fund of Jiangsu Provincial Key Laboratory for Science and Technology of Photon Manufacturing (Jiangsu University GZ201301) and Colleges and Universities in Jiangsu Province plans to graduate research and innovation (CXLX13_168). The authors also thank Dr. Hui Zhang (Testing and Analysis Center, Soochow University) for AFM measurements.

References

[1] Seagle SR. Titanium and titanium alloys. Kirk-othmer encyclopedia of chemical Technology. John Wiley & Sons, Inc; 2000.
[2] Javier Mortensen AL. Metal matrix composites. Annu Rev Mater Res 2010;40(1):243–70.
[3] Bakshi SR, Lahiri D, Agarwal A. Carbon nanotube reinforced metal matrix composites - a review. Int Mater Rev 2010;55(1):41–64.
[4] Singh V, Joung D, Zhai L, Das S, Khondaker SI, Seal S. Graphene based materials: past, present and future. Prog Mater Sci 2011;56(8):1178–271.
[5] Lin D, Saei M, Suslov S, Jin S, Cheng GJ. Super-strengthening and stabilizing with carbon nanotube harnessed high density nanotwins in metals by shock loading. Sci Rep 2015;5:15405.
[6] Lin D, Richard Liu C, Cheng GJ. Laser sintering of separated and uniformly distributed multiwall carbon nanotubes integrated iron nanocomposites. J Appl Phys 2014;115(11):113513.
[7] Lin D, Richard Liu C, Cheng GJ. Single-layer graphene oxide reinforced metal matrix composites by laser sintering: microstructure and mechanical property enhancement. Acta Mater 2014;80:183–93.
[8] Lin D. A laser sintered layer of metal matrix consisting of 0D, 1D and 2D nanomaterials and its mechanical behaviors. Purdue University; 2013.
[9] Balandin AA, Ghosh S, Bao W, Calizo I, Teweldebrhan D, Miao F, et al. Superior thermal conductivity of single-layer graphene. Nano Lett 2008;8(3):902–7.
[10] Novoselov KS, Geim AK, Morozov SV, Jiang D, Zhang Y, Dubonos SV, et al. Electric field effect in atomically thin carbon films. Science 2004;306(5696):666–9.
[11] Lee C, Wei X, Kysar JW, Hone J. Measurement of the elastic properties and intrinsic strength of monolayer graphene. Science 2008;321(5887):385–8.
[12] Dorri Moghadam A, Omrani E, Menezes PL, Rohatgi PK. Mechanical and tribological properties of self-lubricating metal matrix nanocomposites reinforced by carbon nanotubes (CNTs) and graphene – a review. Compos Part B Eng 2015;77:402–20.
[13] Zhai W, Shi X, Yao J, Ibrahim AMM, Xu Z, Zhu Q, et al. Investigation of mechanical and tribological behaviors of multilayer graphene reinforced Ni3Al matrix composites. Compos Part B Eng 2015;70:149–55.
[14] Lee C, Wei X, Li Q, Carpick R, Kysar JW, Hone J. Elastic and frictional properties of graphene. Phys status solidi (b) 2009;246(11–12):2562–7.
[15] Chu K, Jia C. Enhanced strength in bulk graphene-copper composites. Phys status solidi (a) 2014;211(1):184–90.
[16] Bartolucci SF, Paras J, Rafiee MA, Rafiee J, Lee S, Kapoor D, et al. Graphene–aluminum nanocomposites. Mater Sci Eng A 2011;528(27):7933–7.
[17] Tang Y, Yang X, Wang R, Li M. Enhancement of the mechanical properties of graphene–copper composites with graphene–nickel hybrids. Mater Sci Eng A 2014;599:247–54.
[18] Kuang D, Xu L, Liu L, Hu W, Wu Y. Graphene–nickel composites. Appl Surf Sci 2013;273(0):484–90.
[19] Bastwros M, Kim G-Y, Zhu C, Zhang K, Wang S, Tang X, et al. Effect of ball milling on graphene reinforced Al6061 composite fabricated by semi-solid sintering. Compos Part B Eng 2014;60:111–8.
[20] Fadavi Boostani A, Tahamtan S, Jiang ZY, Wei D, Yazdani S, Azari Khosroshahi R, et al. Enhanced tensile properties of aluminium matrix composites reinforced with graphene encapsulated SiC nanoparticles. Compos Part A Appl Sci Manuf 2015;68:155–63.
[21] Cao Y, Zhang J, Feng J, Wu P. Compatibilization of immiscible polymer blends using graphene oxide sheets. ACS Nano 2011;5(7):5920–7.
[22] Xu Z, Gao C. Aqueous liquid crystals of graphene oxide. ACS Nano 2011;5(4):2908–15.
[23] Pan Y, Wu T, Bao H, Li L. Green fabrication of chitosan films reinforced with parallel aligned graphene oxide. Carbohydr Polym 2011;83(4):1908–15.
[24] Pan Z, He L, Qiu L, Korayem AH, Li G, Zhu JW, et al. Mechanical properties and microstructure of a graphene oxide–cement composite. Cem Concr Compos 2015;58:140–7.
[25] Zakharchenko KV, Fasolino A, Los JH, Katsnelson MI. Melting of graphene: from two to one dimension. J Phys Condens Matter 2011;23(20):202202.
[26] Lin D, Suslov S, Ye C, Liao Y, Liu CR, Cheng GJ. Laser assisted embedding of nanoparticles into metallic materials. Appl Surf Sci 2012;258(7):2289–96.
[27] Lin D, Deng B, Sassman SA, Hu Y, Suslov S, Cheng GJ. Magnetic field assisted growth of highly dense α-Fe_2O_3 single crystal nanosheets and their application in water treatment. RSC Adv 2014;4(36):18621–6.
[28] Lin D, Kumar P, Jin S, Liu S, Nian Q, Cheng GJ. Laser direct writing of crystalline Fe_2O_3 atomic sheets on steel surface in aqueous medium. Appl Surf Sci 2015;351:148–54. http://dx.doi.org/10.1016/j.apsusc.2015.05.116.
[29] Lin D, Yang Y, Cheng GJ. Pulsed laser induced confined vapor deposition for thin layer of dense nanoparticle arrays on various substrates. Appl Surf Sci 2013;283:924–9.
[30] Lin D, Ye C, Liao Y, Suslov S, Liu R, Cheng GJ. Mechanism of fatigue performance enhancement in a laser sintered superhard nanoparticles reinforced nanocomposite followed by laser shock peening. J Appl Phys 2013;113(13):133509.
[31] Chen L-Y, Konishi H, Fehrenbacher A, Ma C, Xu J-Q, Choi H, et al. Novel nanoprocessing route for bulk graphene nanoplatelets reinforced metal matrix nanocomposites. Scr Mater 2012;67(1):29–32.
[32] Jeon C-H, Jeong Y-H, Seo J-J, Tien H, Hong S-T, Yum Y-J, et al. Material properties of graphene/aluminum metal matrix composites fabricated by friction stir processing. Int J Precis Eng Manuf 2014;15(6):1235–9.

[33] Xiong D-B, Cao M, Guo Q, Tan Z, Fan G, Li Z, et al. Graphene-and-copper artificial nacre fabricated by a preform impregnation process: bioinspired strategy for strengthening-toughening of metal matrix composite. ACS Nano 2015;9(7):6934–43.
[34] Zan L, Genlian F, Zhanqiu T, Qiang G, Dingbang X, Yishi S, et al. Uniform dispersion of graphene oxide in aluminum powder by direct electrostatic adsorption for fabrication of graphene/aluminum composites. Nanotechnology 2014;25(32):325601.
[35] Pavithra LP, Sarada BV, Rajulapati KV, Rao TN, Sundararajan G. A new electrochemical approach for the synthesis of copper-graphene nanocomposite foils with high hardness. Sci Rep 2014;4:4049.
[36] Gu D, Hagedorn Y-C, Meiners W, Meng G, Batista RJS, Wissenbach K, et al. Densification behavior, microstructure evolution, and wear performance of selective laser melting processed commercially pure titanium. Acta Mater 2012;60(9):3849–60.
[37] Cahoon JR, Broughton WH, Kutzak AR. The determination of yield strength from hardness measurements. MT 1971;2(7):1979–83.
[38] Lin D, Richard Liu C, Cheng GJ. Single-layer graphene oxide reinforced metal matrix composites by laser sintering: microstructure and mechanical property enhancement. Acta Mater 2014;80(0):183–93.
[39] Sadowski P, Kowalczyk-Gajewska K, Stupkiewicz S. Classical estimates of the effective thermoelastic properties of copper–graphene composites. Compos Part B Eng 2015;80:278–90.
[40] Ashby MF, Johnson L. On the generation of dislocations at misfitting particles in a ductile matrix. Philos Mag 1969;20(167):1009–22.
[41] De Cicco M, Konishi H, Cao G, Choi H, Turng L-S, Perepezko J, et al. Strong, ductile magnesium-zinc nanocomposites. Metall Mat Trans A 2009;40(12):3038–45.
[42] Arsenault RJ, Shi N. Dislocation generation due to differences between the coefficients of thermal expansion. Mater Sci Eng 1986;81(0):175–87.
[43] Zhang Z, Chen DL. Consideration of Orowan strengthening effect in particulate-reinforced metal matrix nanocomposites: a model for predicting their yield strength. Scr Mater 2006;54(7):1321–6.
[44] Ganin E, Komem Y, Rosen A. Shock induced hardness in α-Iron. Mater Sci Eng 1978;33(1):1–4.
[45] Casati R, Vedani M. Metal matrix composites reinforced by nano-particles—a review. Metals 2014;4(1):65–83.